J. Chem. Sci. Vol. 128, No. 6, June 2016, pp. 977–989. © Indian Academy of Sciences.
DOI 10.1007/s12039-016-1075-3

Rate coefficients for hydrogen abstraction reaction of pinonaldehyde ($C_{10}H_{16}O_2$) with Cl atoms between 200 and 400 K: A DFT study

G SRINIVASULU and B RAJAKUMAR*
Department of Chemistry, Indian Institute of Technology Madras, Chennai 600 036, India
e-mail: rajakumar@iitm.ac.in

MS received 18 November 2015; revised 14 February 2016; accepted 13 March 2016

Abstract. The kinetics of the reaction between pinonaldehyde ($C_{10}H_{16}O_2$) and Cl atom were studied using high level *ab initio* G3(MP2) and DFT based MPWB1K/6-31+G(d) and MPW1K/6-31+G(d) levels of theories coupled with Conventional Transition State Theory in the temperature range between 200 and 400 K. The negative temperature dependent rate expression for the title reaction obtained with Wigner's and Eckart's symmetrical tunneling corrections are $k(T)=(5.1 \pm 0.56) \times 10^{-19} T^{2.35} \exp[(2098 \pm 2)/T]$ cm^3 molecule^{-1} s^{-1}, and $k(T)=(0.92 \pm 0.18) \times 10^{-19} T^{2.60} \exp[(2204 \pm 4)/T]$ cm^3 molecule^{-1} s^{-1}, respectively, at G3(MP2)//MPWB1K method. The H abstraction reaction from the –CHO group was found to be the most dominant reaction channel among all the possible reaction pathways and its corresponding rate coefficient at 300 K is $k_{(\text{Eckart's unsymmetrical})} = 3.86 \times 10^{-10}$ cm^3 molecule^{-1} s^{-1}. Whereas the channel with immediate lower activation energy is the H-abstraction from –CH- group (Tertiary H-abstraction site, C_g). The rate coefficient for this channel is $k_{Cg(\text{Eckart's unsymmetrical})} = 1.83 \times 10^{-15}$ cm^3 molecule^{-1} s^{-1} which is smaller than the dominant channel by five orders of magnitude. The atmospherically relevant parameters such as lifetimes were computed in this investigation of its reaction with Cl atom.

Keywords. Pinonaldehyde; MPWB1K; Kinetics; G3(MP2); rate coefficient; atmospheric lifetime.

1. Introduction

The large variety of volatile non-methane organic compounds and biogenic volatile organic compounds (BVOCs) are emitted into the atmosphere mainly from vegetation,[1–5] and they have received enormous attention. These BVOCs include isoprene, $C_{10}H_{16}$ monoterpenes, ($C_{15}H_{24}$) sesquiterpenes, and a number of oxygenated compounds. α and β Pinene are the most abundant among the other monoterpenes released into the atmosphere. Pinonaldehyde (3-Acetyl-2,2-dimethylcyclobutaneacetaldehyde) is a low volatile product of the atmospheric reactions of α-pinene.[6]

The global average (24 h) (Singh *et al.*[7]) concentration of Chlorine (Cl) atom is around or below 10^4 cm^{-3} and the concentration of Cl atom, within the broad range of literature values ranging from 10^4 to 10^6 cm^{-3} (Graedel and Keene[11]) in the Marine Boundary Layer (MBL).[7–11] There is increasing interest in understanding the potential of chlorine atoms contributing to tropospheric chemistry in the marine boundary layer and in coastal regions.[12–14] Atomic chlorine is highly reactive with a variety of organic and inorganic compounds,[15–17] therefore, relatively small concentrations can compete with the OH radical, O_3 and NO_3, in determining the tropospheric fate of such compounds. Since the reactions of organic compounds with chlorine (Cl) atoms are typically about 10 times faster than the corresponding OH radical reactions, Cl atoms play a very important role in the removal of organic compounds from the lower troposphere.

The reactions of pinonaldehyde with OH, O_3 and NO_3 were reported in the literature.[6,18–21] However, only one investigation[22] on Cl atom reaction is available, to the best of our knowledge. Nozière *et al.*,[22] carried out the reaction at 298 K using relative rate methods with analytical techniques such as FTIR spectroscopy and gas chromatography. They have reported the rate coefficient for the title reaction at the room temperature to be k (Pinonaldehyde + Cl)=$(2.4 \pm 1.4) \times 10^{-10}$ cm^3 molecule $^{-1}$ s^{-1}. Temperature dependent rate coefficients for this reaction are not available in the literature till date.

The temperature dependent rate coefficient, k in the range of 200 to 400 K for the reaction of Cl atom with pinonaldehyde (labelling of the different C-sites represented below in R1), which is a significant removal process in the MBL, using computational methods was studied for the first time. In addition, the cumulative atmospheric lifetimes of pinonaldehyde due to its

*For correspondence

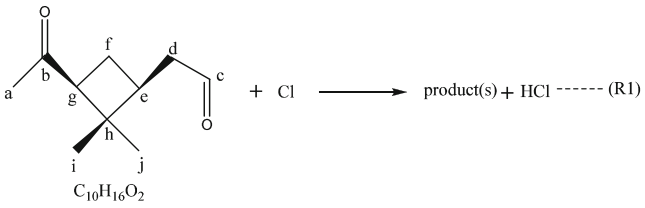

Scheme 1. Reaction of title compound with Cl atom.

reactivity with both OH radicals and Cl atoms were computed in this study (scheme 1).

2. Computational Methods

2.1 *Quantum chemical methods*

In the present study, the geometries of the reactants namely, pinonaldehyde ($C_{10}H_{16}O_2$) and chlorine atom (Cl), adduct (TSc_{ADD}), transition states (TSs), product complex (PCc) and products (P) were optimized with hybrid density functional theory, namely MPW1K[23] and hybrid meta density functional theory, called MPWB1K[24] using a Pople basis set with diffuse functions 6-31+g(d), which is available internally in the Gaussian program suite.[25] In recent articles it is shown that the density functional theories (DFT) are specifically developed for kinetics and thermochemistry and are known to produce reliable results.[26–28] The MPWB1K functional, which was developed for kinetic calculations, has been shown to be more accurate than previously introduced MPW1K functional.[24] To get reliable reaction energies and barrier heights, single-point calculations for the stationary points are carried out at G3(MP2)[29] method using the optimized geometries obtained at MPW1K and MPWB1K functional. This kind of dual level procedures are known to produce reliable kinetic and thermochemical parameters. In the recent past, similar reactions were studied in our group by optimizing the structural parameters using MP2 and DFT theories and then energies were refined using high level *ab initio* methods.[42] The optimized structures are given in figure 1, and the structural parameters are given in table S-I in the Supporting Information (SI). The oxidation of pinonaldehyde by chlorine atom is initiated by H-atom abstraction at different C-sites. All the transition states (TSa1, TSa2, TSa3, TSc, TSd1, TSd2, TSe, TSf1, TSf2, TSg, TSi1, TSi2, TSi3, TSj1, TSj2 and TSj3) correspond to the abstraction of hydrogen by chlorine atom

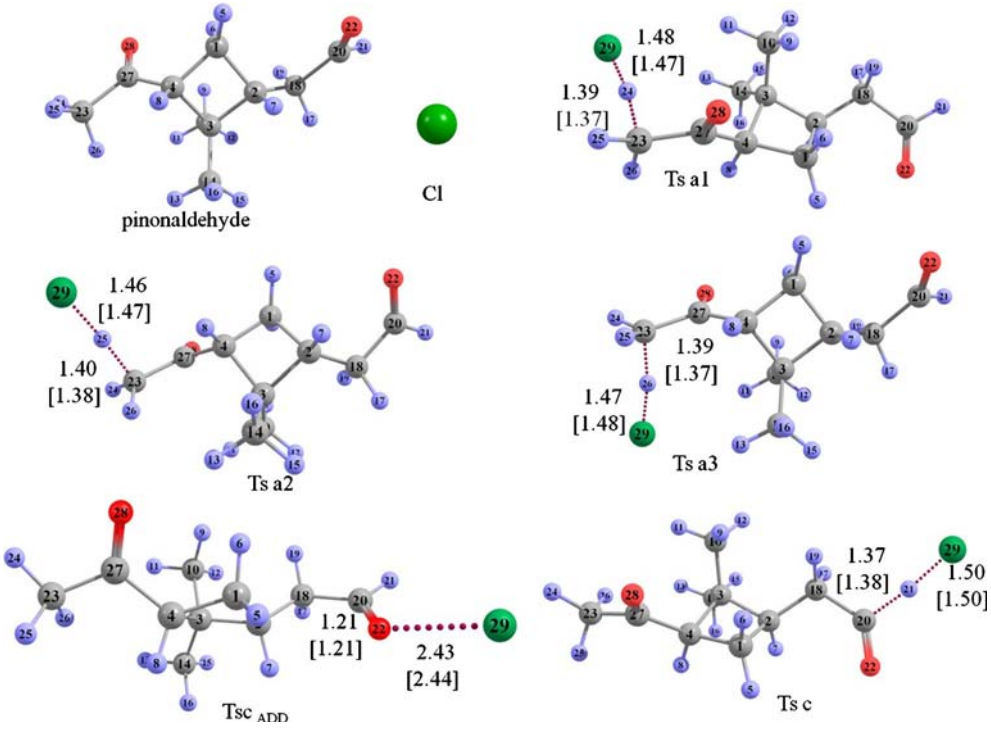

Figure 1. Optimized geometries of the reactants, adduct, product complex, all transition states and all the products were obtained at MPWB1K/6-31+G(d), MPW1K/6-31+G(d) (in parentheses) levels of theory. Bond lengths are given in Å. Violet color represents hydrogen, grey color represents carbon; red color represents oxygen atom, and green color represents chlorine atom in the structures.

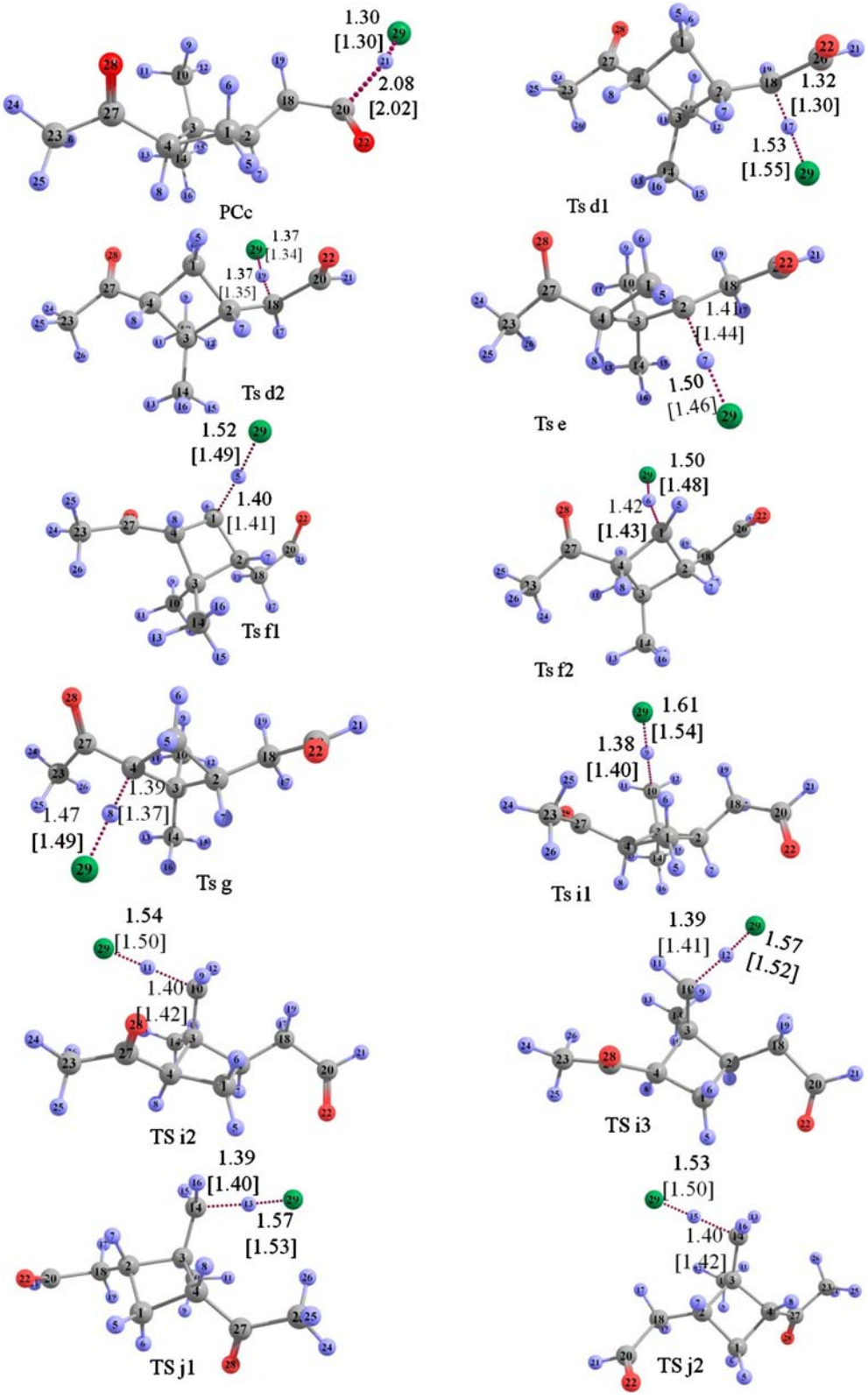

Figure 1. (*continued*)

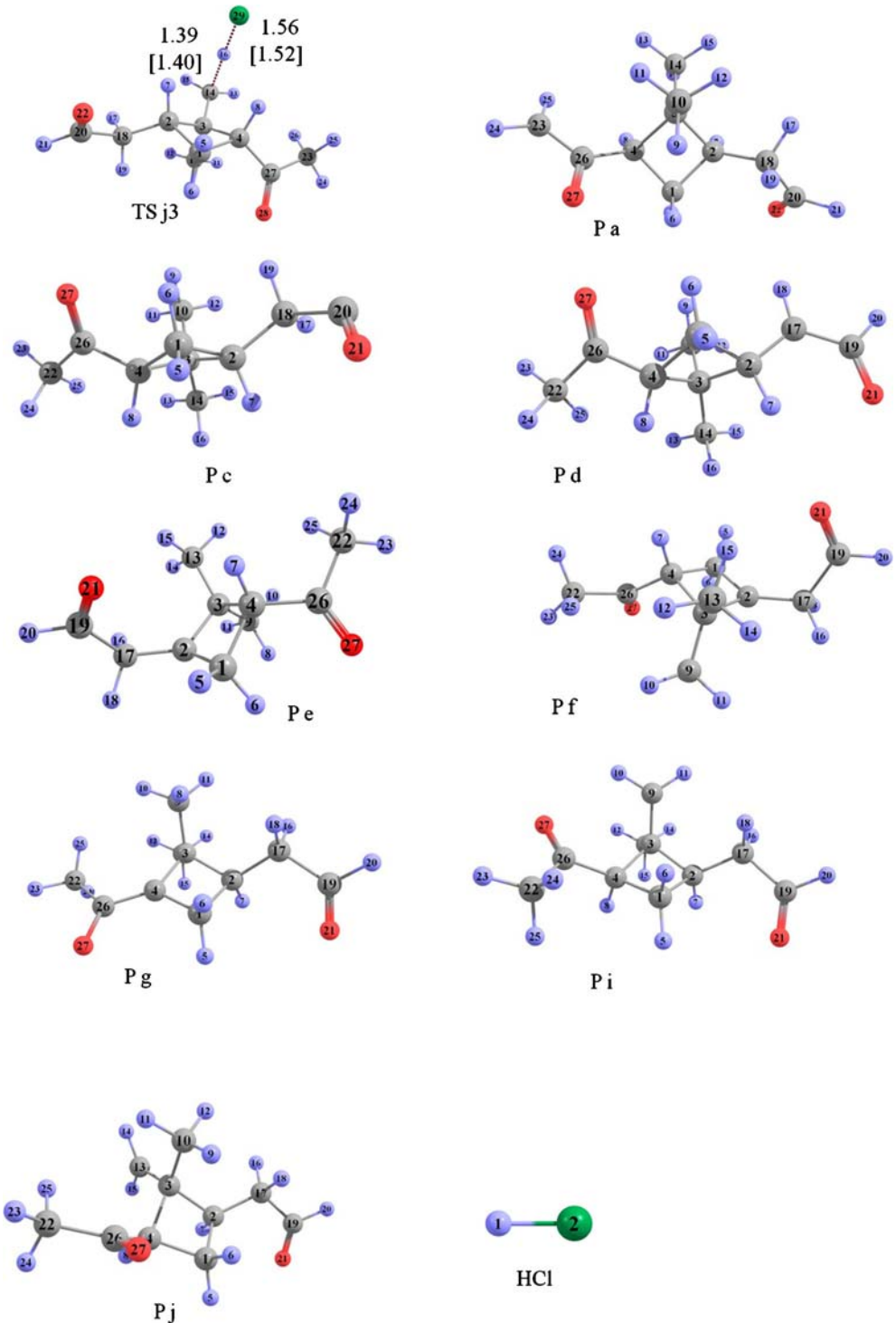

Figure 1. (*continued*)

from different C-sites in pinonaldehyde, are shown in table 1. The subscripts a, c, d, e, f, g, i and j correspond to the abstraction of H atom from the corresponding C-sites. The vibrational frequencies of all the standard states were calculated and are given in table S2 (in SI). All the optimized geometries of the reactants, adduct, product complex and products were confirmed with zero imaginary frequency (NImag = 0) and TSs were confirmed with one imaginary frequency (NImag = 1).

Larger spin contamination may lead to a poor estimation of the barrier height. Therefore, in the present investigation, the spin contamination before and after annihilation for all systems which are involved in the title reaction are reported. The spin contamination

Table 1. Hydrogen abstraction by Cl atom from C-sites in pinonaldehyde and corresponding transition states.

H-abstraction site	Transition states
Ca	Tsa1,Tsa2, Tsa3
Cc	TSc
Cd	TSd1,TSd2
Ce	Tse
Cf	TSf1,TSf2
Cg	TSg
Ci/j	Tsi1,Tsi2,Tsi3 and TSj1,TSj2,TSj3

before annihilation was found to be in the range of 0.75 to 0.78, and after annihilation, the $<S^2>$ value is 0.75; the optimized values of $<S^2>$ for all the transition states at both levels of theories are given in table S5 (in SI). Structural parameters for the title reaction obtained at MPW1K/6-31+G(d) and MPWB1K/6-31+G(d) were used for the refinement of energies and kinetic calculations.

All the calculations were carried out using Gaussian 09 program suite[25] and the normal modes of reactants, adduct, transition states, product complex and products are viewed in Gauss View.[30]

2.2 *Kinetic methods*

Rate coefficients for the title reaction (pinonaldehyde + Cl) were calculated using the conventional transition state theory (CTST).[31]

$$k\,(T) = \sigma \frac{k_B T}{h} \left(\frac{Q_{\ddagger}}{Q_R}\right) exp\left(\frac{-\Delta E_0^{\ddagger}}{RT}\right) \qquad (1)$$

Here, σ is the reaction path degeneracy, ‡ represents the transition state, k_B is Boltzmann constant, h is Planck's constant, T is temperature in Kelvin, $Q_{\ddagger}$ and Q_R are the partition functions for the transition states and reactants, respectively. $\Delta E_0^{\ddagger}$ is the barrier height, and R is gas constant. The two spin-orbit (SO) states $^2p_{3/2}$ (lowest) and $^2p_{1/2}$ of Cl having degeneracies of 4 and 2, respectively, and separated by 882.3515 cm^{-1},[32] were included in the electronic partition function calculations. Quantum mechanical tunnelling effects along the reaction coordinates are included by temperature dependent transmission coefficient Γ (T). The values of Γ (T) were calculated by using three methods namely Wigner's method[33] and Eckart's symmetrical and unsymmetrical tunneling method.[34–36] The Wigner's tunneling correction factors were calculated using the imaginary frequency of the transition states and the Eckart's symmetrical tunnelling correction factors were calculated using the imaginary frequency of the transition state and also zero-point corrected barrier heights. In case of all TSs, both forward barrier from reactants (R) to TS and backward barrier from products (P) to TS were used for Eckart's unsymmetrical tunneling corrections. In the case of TSc, which is a submerged TS, the tunneling corrections were performed through a complex mechanism (R→Adduct→TS→PC→P), as adduct and product complexes play very important roles in tunneling. The CTST coupled with Wigner's and Eckart's tunneling methods were used in previous articles by our group[37–42] and by various other groups[43–46] and those studies showed reasonably accurate results when compared with the experimentally measured ones for the H abstraction reactions by various radicals. For example, in the case of H-atom abstraction reaction by OH radical from pinonaldehyde,[42] theoretically computed rate coefficients at 300 K with G3(MP2) theory using Wigner's method; symmetrical and unsymmetrical Eckart's tunneling corrections are 3.69×10^{-11}, 4.72×10^{-11}, and 3.78×10^{-11} $cm^3 molecule^{-1} s^{-1}$, respectively. The computed rate coefficients at 300 K are in good agreement with the experimentally measured rate coefficients, $(3.46 \pm 0.4) \times 10^{-11}$ cm^3 $molecule^{-1} s^{-1}$ at 297 K by Davis *et al.*,[18] $(4.8 \pm 0.8) \times 10^{-11}$ cm^3 $molecule^{-1}$ s^{-1} at 296 K by Alvarado *et al.*,[20] and $(4.0 \pm 1.0) \times 10^{-11}$ cm^3 $molecule^{-1}$ s^{-1} at 293 K by Nozière *et al.*[22] It should be noted here that, the present computed results at all different tunneling corrections are in good agreement with the reported literature values. TST calculations were carried out using two models, namely harmonic oscillator (HO) and hindered rotor (HR) models. To account for quantum mechanical hindered rotor corrections in the rate coefficient calculations, pinonaldehyde and corresponding transition states were optimized at the MPWB1K level of theory. The torsional motion of the bonds C(2)—C(18), C(18)—C(20) and C(4)—C(27) were treated with either harmonic oscillator (HO) or Hindered Rotor (HR) models for the calculations of pre-exponential factors. Two or three lower frequencies of the reactant and all the TSs were treated as hindered rotors and the other vibrational frequency modes were treated as separable harmonic oscillators. The highest torsional barrier was observed to be 1.28 kcal mol^{-1}, in the case of C(4)—C(27) bond. All the lower vibrational frequencies of the pinonaldehyde and all the TSs and the corresponding calculated torsional barriers are given in table S3 in the Supporting information (SI). In general, when the bond length in the transition state increases, the torsional barrier decreases. It should be noted here that this effect, as the C-C bond lengths in the transition states are slightly longer than the corresponding bonds in pinonaldehyde and therefore, the rotational barriers of the transition states are lower than those of pinonaldehyde. Therefore,

the hindered rotor corrections for rotation (along C-C bond) of $COCH_3$, CH_2CHO and CHO groups of the reactant and transition states were accounted for the rate coefficient calculations. The method proposed by Truhlar and co-workers,[47] was used in our calculations, for HR model. Rate coefficients were obtained in the range of temperatures, 200-400 K, with an interval of 25 K.

3. Results and Discussion

3.1 *Energetics and Quantum chemical calculations*

Figure 1 presents the stationary geometries of the reactants, adduct (TSc_{ADD}), TSs, product complex (PCc) and products, obtained at MPW1K/6-31+G (d) and MPWB1K/6-31+G (d) levels of theory. As shown in figure 1, the optimized parameters, which are obtained at the two levels, are reasonably close to each other. The potential energy surfaces (PES) based on the energies obtained at the G3(MP2)//MPWB1K/6-31+G(d) level of theory are plotted in figure 2. The barrier heights $\Delta E_0^{\ddagger}$ and entropy of activation $\Delta S_0^{\ddagger}$ for abstraction of each and every H atom from pinonaldehyde ($C_{10}H_{16}O_2$) by Cl atom were computed and listed in table 2. The reaction was observed to follow two pathways. In one pathway, the energies of all TSs are higher than the reactants and in case of other pathway, barrier energy for one transition state, namely, TSc is lower than the reactants. This transition state (TSc) alone, which is a submerged one, is found to be governing the total reaction based on present calculations, which show negative temperature dependence. A reaction complex is expected for the transition state (TSc), which is lower in energy than the reactants. However, when we tried to optimize such a reaction complex, a stable adduct between the Cl atom and the oxygen atom of the >C=O in the aldehyde was found. In the case of formaldehyde and acetaldehyde reactions with Cl atom, the possibility of formation of such type of stable adducts have been reported in the literature by Gruber-Stadler *et al*.,[48] and Beukes *et al*.[49] They have mentioned in their articles that this kind of adducts are quite possible for higher aldehydes as well. In agreement with the above authors, the adduct (−4.65 kcal mol^{-1}) formed between Cl atom and oxygen atom of >C=O group was found in the present study. Here, the structure and the energy of this stable adduct (−4.65 kcal mol^{-1}) and product complex (-16.97 kcal mol^{-1}) formed between pinonaldehyde and the newly formed HCl molecule are reported and they are shown in figures 1 and 2. The $\Delta H_{formation}$ of the HCl-pinonaldehyde complex is -17.16 kcal mol^{-1} and $\Delta H_{reaction}$ is −14.20 kcal mol^{-1}.

The elongation of the breaking C-H bond lengths were found to vary between 17% and 32% and the

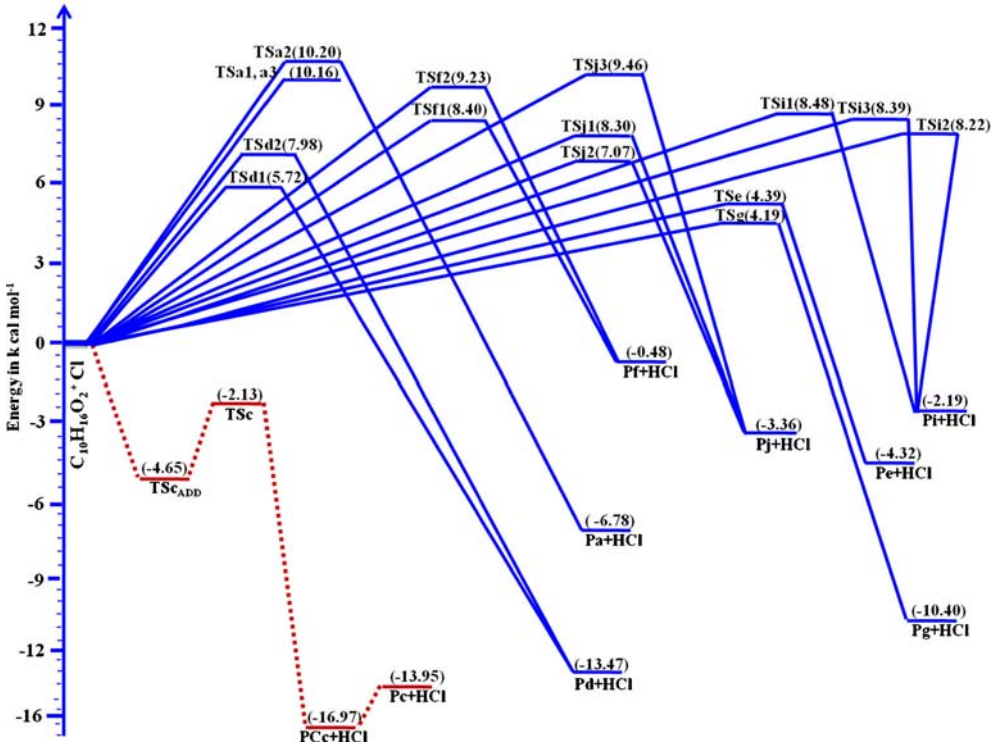

Figure 2. Schematic potential energy diagram for the reaction through all the transition states obtained at G3(MP2)//MPWB1K/6-31+G(d) level of theory. The relative energies are given in the units of kcal mol^{-1}.

Table 2. Barrier heights ($\Delta E_0^{\ddagger}$ in kcal mol^{-1}), entropy of activation ($\Delta S^{\#}$ (298 K) cal mol^{-1} K^{-1}) and rate coefficients (cm^3 molecule^{-1} s^{-1}) of each transition state (at 300 K) obtained at various levels of theory.

	$\Delta E_0^{\ddagger}$		$\Delta S^{\ddagger}$(298 K)		$k_{(Eckartsunsymm)}$ at 300 K	
TS	G3(MP2)// MPW1K	G3(MP2)// MPWB1K	G3(MP2)// MPW1K	G3(MP2)// MPWB1K	G3(MP2)// MPW1K	G3(MP2)// MPWB1K
TSa1	8.29	10.16	−27.12	−29.14	2.75×10^{-18}	1.40×10^{-19}
TSa2	8.39	10.20	−25.43	−23.03	3.44×10^{-18}	1.62×10^{-17}
TSa3	8.29	10.16	−27.12	−29.13	2.75×10^{-18}	1.40×10^{-19}
TSc	−4.30	−2.13	−23.34	−22.96	1.85×10^{-9}	3.86×10^{-10}
TSd1	3.84	5.72	−25.79	−26.33	5.72×10^{-16}	3.57×10^{-16}
TSd2	6.07	7.98	−25.11	−25.12	6.15×10^{-17}	4.04×10^{-17}
TSe	2.55	4.39	−24.93	−23.80	1.89×10^{-15}	8.58×10^{-15}
TSf1	6.45	8.40	−22.06	−24.34	6.46×10^{-17}	9.44×10^{-18}
TSf2	6.45	9.23	−25.78	−27.90	2.03×10^{-18}	6.97×10^{-19}
TSg	2.38	4.19	−25.51	−25.66	1.12×10^{-15}	1.83×10^{-15}
TSi1	6.55	8.68	−27.28	−28.99	1.15×10^{-18}	4.52×10^{-19}
TSi2	6.36	8.22	−26.16	−26.86	1.48×10^{-18}	9.02×10^{-19}
TSi3	6.35	8.39	−25.35	−24.58	1.49×10^{-18}	3.69×10^{-18}
TSj1	6.21	8.30	−25.74	−26.32	1.18×10^{-17}	2.52×10^{-18}
TSj2	5.16	7.07	−25.52	−27.52	3.01×10^{-17}	1.41×10^{-18}
TSj3	7.43	9.46	−24.60	−24.83	5.45×10^{-18}	8.32×10^{-19}

Table 3. Heat of reaction [ΔH^0 (298 K) in kcal mol^{-1}], Gibbs free energy [ΔG^0 (298 K) in kcal mol^1] and entropy of reaction [ΔS^0 (298 K) in cal mol^{-1} K^{-1}] for the reaction between Cl atom and pinonaldehyde at different levels of theory.

	ΔH^0(298 K)		ΔG^0(298 K)		ΔS^0(298 K)	
H-abstraction site	G3(MP2)// MPW1K	G3(MP2)// MPWB1K	G3(MP2)// MPW1K	G3(MP2)// MPWB1K	G3(MP2)// MPW1K	G3(MP2)// MPWB1K
Ca	−7.26	−7.26	−9.01	−9.01	14.95	14.95
Cc	−14.20	−14.20	−16.64	−16.64	8.21	8.21
Cd	−13.80	−13.80	−16.38	−16.37	8.64	8.64
Ce	−4.33	−4.33	−7.68	−7.68	11.23	11.23
Cf	−0.60	−0.60	−3.29	−3.29	9.01	9.01
Cg	−10.51	−10.51	−13.21	−13.21	9.04	9.04
Ci	−2.20	−2.20	−5.20	−5.20	10.07	10.07
Cj	−3.33	−3.31	−6.29	−6.29	9.93	9.93

forming H...Cl bonds were found to vary between 8% and 17%. These bond lengths are longer than the normal C-H and H-Cl bond lengths in pinonaldehyde and in HCl, respectively. In all reaction channels the elongation of breaking bond (C-H) is less than that of the forming bond (H-Cl), indicating that these transition states are all reactant-like, *i.e*., the reaction will proceed through an "early" transition state which is expected for an exothermic reaction path.

3.2 *Comparison of Methods*

The energetics of the title reaction such as barrier heights, the standard enthalpy change (ΔH^0), standard free energy change (ΔG^0), and standard entropy change (ΔS^0) for all the H-abstraction reaction channels are given in tables 2 and 3. It is observed that the MPWB1K functional provides better estimation of barrier heights than the MPW1K method. To refine the barrier heights, the structural parameters obtained at MPWB1K were used with *ab initio* G3(MP2) method. This *ab initio* method has successfully minimized the error from the correlation of electrons and "spin contamination effect". The obtained barrier heights are shown in table 2 for the title reaction. From table 2, it is very clear that the G3MP2//MPWB1K theory provides better results with negative barrier height. For example, the barrier for TSc was predicted to be −2.13 kcal mol^{-1} with G3(MP2)/MPWB1K and it was −4.30 kcal mol^{-1} with G3(MP2)//MPW1K. Unfortunately there are no studies available in the literature on the title reaction, to compare the kinetic parameters computed in this study.

From table 2 it is very clear that the E_a values obtained using MPW1K theory are ~2 kcal mol^{-1} lower than those estimated using MPWB1K theory. In addition to this, it should be indicated here that $\Delta S^{\ddagger}$ values obtained using both the theories are in good agreement with each other. Given this scenario, certainly this would lead to the overestimation of the rate coefficients in the case of MPW1K theory when compared with MPWB1K theory. Here it should be noted again that, this comparison is made based on the available experimentally measured rate coefficients only. Also the calculated rate coefficients, at the G3MP2//MPWB1K/6-31+G (d) method, are in good agreement with experimentally reported rate coefficients and with the estimated ones using structure activity relationship (SAR) data as well.

As summarized in table 3, both MPWB1K and MPW1K density functional methods are appropriate to determine thermochemical properties like enthalpy change, free energy change and entropy change in comparison with ab initio methods. As shown in table 3, the calculated thermodynamic properties of both the DFT methods are in excellent agreement with each other.

Reaction going through the aldehydic H-abstraction site (C_c) was found to be more exothermic (-14.20 kcal mol^{-1}) than ketonic H-abstraction site (C_a) and all other abstraction sites (Ce, Cf, Cg, Ci and Cj) as well. Among the two tertiary H- abstraction sites (C_e and C_g), it is very clear that H-abstraction from C_g site is found to be more exothermic (-10.51 kcal mol^{-1}) than C_e site (-4.33 kcal mol^{-1}). In the case of H- abstraction from C_d site (-13.80 kcal mol^{-1}), it is found to be more exothermic than the other C-sites (except C_c site) and it may be due to the fact that C-H bond strength at C_d carbon is lower than the C-H bond strengths at other C-sites. The H-abstraction from C_f, C_i and C_j sites have shown approximately identical exothermicities -0.60, -2.20 and -3.33 kcal mol^{-1}, respectively. In conclusion, both MPW1K and MPWB1K methods are found to be good for obtaining thermodynamic properties for this reaction.

3.3 *Rate coefficient calculations*

Only one experimental study is available for the title reaction at 298 K in the literature. Neither temperature dependent experimental studies nor theoretical studies are reported for the title reaction till date. In the present theoretical investigations, the rate coefficients for the reaction of Cl atoms with pinonaldehyde were calculated using CTST in the temperature range of 200-400 K. The rate coefficients were computed by taking the barrier energies for all TSs, through direct mechanism (R→TS→P) expect for TSc, submerged TS. In case of the reaction channel going through the submerged TS, Alvarez-Idaboy *et al.*,[50,51] and Galano *et al.*,[52] have proposed a complex mechanism (R→RC→TS→PC→P), which is similar to the one proposed in this study (R→Adduct→TS→PC→P). The rate coefficients obtained using this method, are in very good agreement with the reported (experimental) rate coefficient at room temperature. Here it should be emphasized that J.R. Alvarez-Idaboy *et al.*,[50,51] have calculated rate coefficients for reaction of HCHO with OH radical using direct mechanism (R→TS→P) and complex mechanism (R→RC→TS→PC→P). The obtained rate coefficients are 0.19×10^{-11} and 1.10×10^{-11} cm^3 $molecule^{-1}s^{-1}$, respectively. In the case of CH_3CHO+OH reaction, the obtained rate coefficient through direct mechanism is 0.59×10^{-11} cm^3 $molecule^{-1}$ s^{-1} and through complex mechanism it is 1.45×10^{-11} cm^3 $molecule^{-1}s^{-1}$. In both the cases rate coefficients obtained through complex mechanism are found to be in excellent agreement with the experimentally reported values of the respective reactions.

The forward barrier height from intermediates (TSc_{ADD}) to TS (known as effective barrier Eeff = E_{TS}-E_{TSCADD}) was used for Eckart's symmetrical tunneling corrections. Both the forward barrier from TSc_{ADD} to TS and the backward barrier from PC to TS were used for Eckart's unsymmetrical tunneling corrections. At high pressures one can assume that these complexes are in equilibrium with the reactants. When the magnitude of tunneling is calculated using the Eckart's model, it does matter what the barrier height is, if it is measured from the bottom of the well or from the energy level of the non-interacting reactants. In these calculations the barrier heights are measured from the bottom of the well of TSc_{ADD}. As mentioned earlier, out of total sixteen independent transition states, two transition states, namely, TSa1 and TSa3 are symmetrically equivalent. Since pinonaldehyde is quite a floppy molecule and it has no rigid structure that would demand a separate treatment for each H atom. In the methyl groups at least two H-atoms are very similar and are separated by very low barrier heights. So it would be more reasonable to treat them as identical transition states (TSa1 and TSa3) with reaction path degeneracy (σ). Therefore, $\sigma = 2$ was used in present rate coefficients calculations. Whereas, in case of rest of the TSs, corresponding hydrogens are non-equivalent. Therefore, in the current investigation they were treated as independent TSs.

The transition state TSc was found to be a submerged one, whose energy is lower than the reactants. It is expected that, the submerged transition state would contribute more to the total rate coefficient and

dominate the complete reaction when compared with positive barrier transition states, as given in table 2. Pinonaldehyde has one aldehydic and one ketonic H atoms. The bond dissociation energies for hydrogen which are connected to both carbonyl groups in pinonaldehyde were calculated. The Bond dissociation energies of C-H bond of aldehydic H atom in R-C(=O)-H group and ketonic functional group R-C(=O)-CH_3 in pinonaldehyde molecule are given table S4 (in Supporting Information). In addition, these parameters were compared with those of acetaldehyde and acetone. From the table S4, it is clear that the bond dissociation energy for the H atom connected to carbon C_a obtained at MPWB1K theory is 90.57 kcal mol^{-1}. This is in very good agreement with the reported[53] bond dissociation energy (92.82 kcal mol^{-1}). This energy is similar even in case of acetone (93.36 kcal mol^{-1}). Whereas, the bond dissociation energy of aldehydic hydrogen on carbon C_c obtained at MPWB1K level of theory is 84.29 kcal mol^{-1}. This value is in good agreement with the reported one (85.55 kcal mol^{-1})[53] which is again very close to that of acetaldehyde (87.43 kcal mol^{-1}). It is very obvious that the BDEs for the aldehydic H atoms are lower than those of the ketonic H atoms. Therefore, H-abstraction from the aldehydic H-abstraction site (C_c) should predominate the reaction. This conclusion can be further verified by rate coefficient data given in the table S4.

In case of a barrierless reaction, the variational effects on the rate coefficient may expected to be significant. In case of H abstraction by OH radicals from pinonaldehyde,[42] the variational effects of submerged transition states with the similar barriers were found not to be important. In our earlier paper on pinonaldehyde[42] the reaction path analysis was explored and classical potential energy curve (V_{MEP}), vibrational ground-state adiabatic potential energy (V_A^G), and zero-point energy (ZPE) curve as functions of reaction coordinate, where $V_a^G = V_{MEP}+ZPE$, were reported. Based on those results, we have noticed that, V_{MEP} and V_a^G curves are similar in shape (cf from figure 3, Reference 42), and the maximum values of V_{MEP} and V_a^G are located approximately at the same position on the reaction path, that is, at $s = 0$. The ZPE, which is difference between V_a^G and V_{MEP}, shows a little change near the saddle point. Based on these observations one can conclude that for the reaction of pinonaldehyde with OH radical or Cl atom, the variation effect is small or almost negligible. Furthermore, several research groups[54–56] including our group[42,57] have followed the same kind of approach for H-abstraction reactions of various molecules. No significant difference was observed between computed rate coefficients

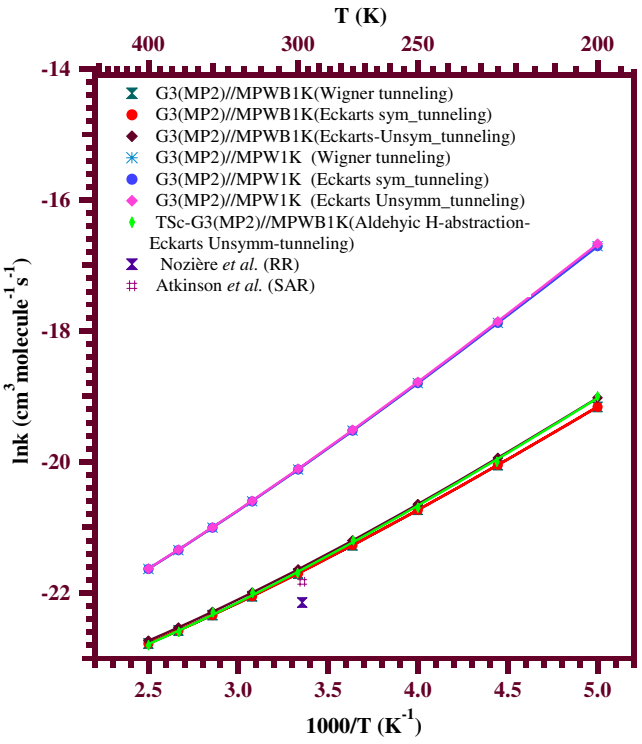

Figure 3. Arrhenius plot of the rate coefficient data obtained for the Cl atom reaction with pinonaldehyde over the temperature range of 200–400 K. The data are identified by different symbols and are defined therein. (RR-Relative Rate technique, SAR- Structure Activity Relationship).

obtained at CVTST (canonical variational transition-state theory) and CTST methods. Therefore, CVTST calculations were not performed and only CTST calculations were carried out in the present investigation.

It is clear from table 2, that the submerged transition state TSc is lying lower in energy than the reactants by about −2.13 kcal mol^{-1}. It is obvious that TSc (H-abstraction from –CHO group) is much more stabilized than the rest of the transition states. The total rate coefficient is obtained by summing all the rate coefficients for the reaction going through all TSs. The computed rate coefficients for the title reactions are plotted in figure 3. The data were fit to the Arrhenius equation using a three-parameter fit, in the studied temperature range of 200–400 K. To our surprise, the computed rate coefficients obtained from the Eckart's and Wigner's symmetrical tunneling correction are equal at both levels of theory. The Arrhenius expressions obtained from the computed rate coefficients at MPW1K and MPWB1K levels of theory in the range of 200–400 K are $k(T)=(1.52 \pm 0.11) \times 10^{-18}T^{2.16}\exp[(2571 \pm 2)/T]$ cm^3 $molecule^{-1}$ s^{-1} and $(5.1 \pm 0.56) \times 10^{-19}T^{2.3}\exp[(2098 \pm 2)/T]$ cm^3 $molecule^{-1}$ s^{-1}, respectively. To the best of our knowledge, Arrhenius

parameters for this reaction are not available in any temperature range. The computed rate coefficients for the H- abstraction reaction of pinonaldehyde by chlorine atom using Eckart's tunneling and Wigner's tunneling methods with the G3(MP2)//MPW1K and G3(MP2)//MPWB1K levels of theory using the HR model over the temperature range from 200 to 400 K are given in table 4, and depicted in figure 3, as well. Whereas, when Eckart's unsymmetrical tunneling corrections are employed, the Arrhenius expressions obtained from the computed rate coefficients at MPW1K and MPWB1K levels of theory in the temperature range of 200-400 K are $k(T)=(6.51 \pm 0.54) \times 10^{-19} T^{2.28} \exp[(2616 \pm 2)/T]$ $cm^3 molecule^{-1} s^{-1}$ and $k(T)=(0.92 \pm 0.18) \times 10^{-19} T^{2.60} \exp[(2204 \pm 4)/T]$ cm^3 $molecule^{-1} s^{-1}$, respectively. The theoretically calculated rate coefficients in the present work have shown negative temperature dependence over the studied temperature range. The fit parameters obtained using both HO and HR models are given in table 5.

As shown in table 4, at 300 K, the computed rate coefficients obtained with G3(MP2)//MPWB1K theory using Eckart's symmetrical, Wigner's tunneling corrections are equal ($3.75 \times 10^{-10} cm^3$ $molecule^{-1}$ s^{-1}) and this is 1.5 times higher than the reported rate coefficient by Nozière *et al.,* [22] $(2.4 \pm 1.4) \times 10^{-10}$ $cm^3 molecule^{-1}$ s^{-1}. The computed rate coefficients obtained at 300 K with G3(MP2)//MPWB1K theory using Eckart's unsymmetrical tunneling correction is $3.86 \times 10^{-10} cm^3$ $molecule^{-1}$ s^{-1}, which is 1.6 times higher than the reported one. It should be noted here that the rate coefficients obtained using Eckart's symmetrical and unsymmetrical methods are very close to each other. At lower temperatures, (table 4, T<250 K), obtained rate coefficients are higher than the collision rate limit $\sim 8 \times 10^{-10}$ cm^3 $moecule^{-1} s^{-1}$, which suggest that the reaction proceeds faster than a collision. This could only happen when ions are involved, which is not the case here. The possible reason behind this behavior could be the inherent limitation methodology/theory used to compute these rate coefficients.

Table 4. Rate coefficients ($cm^3 molecule^{-1} s^{-1}$) for pinonaldehyde + Cl reaction in the temperature range of 200-400 K at various levels of theory.

	Rate coefficients[a]		Eckart unsymmetrical		
Temperature	G3(MP2)// MPW1K	G3(MP2)// MPWB1K	G3(MP2)// MPW1K	G3(MP2)// MPWB1K	Reported rate coefficient k (298 K)
200	5.53×10^{-08}	4.76×10^{-09}	5.74×10^{-08}	5.36×10^{-09}	[b]2.4×10^{-10} (RR)
225	1.71×10^{-08}	1.96×10^{-09}	1.75×10^{-08}	2.12×10^{-09}	[c]3.3×10^{-10}(SAR)
250	6.86×10^{-09}	9.89×10^{-10}	6.97×10^{-09}	1.04×10^{-09}	[b]Nozière *et al.*
275	3.31×10^{-09}	5.77×10^{-10}	3.35×10^{-09}	6.00×10^{-10}	[c]Atkinson
300	1.83×10^{-09}	3.75×10^{-10}	1.85×10^{-09}	3.86×10^{-10}	
325	1.13×10^{-09}	2.64×10^{-10}	1.14×10^{-09}	2.71×10^{-10}	
350	7.53×10^{-10}	1.98×10^{-10}	7.57×10^{-10}	2.02×10^{-10}	
375	5.36×10^{-10}	1.57×10^{-11}	5.38×10^{-10}	1.59×10^{-10}	
400	4.02×10^{-10}	1.29×10^{-11}	4.03×10^{-10}	1.30×10^{-10}	

[a]The rate coefficients obtained using both the tunneling methods (Eckart's symmetrical and Wigner's methods) are identical.
[b] Nozière *et al.*[22]
[c]Atkinson *et al.*[58,59]

Table 5. Arrhenius parameters obtained for the title reaction $C_{10}H_{16}O_2$+Cl at various levels of theory.

					Eckart's unsymmetrical tunneling corrections			
	G3(MP2)//MPW1K		G3(MP2)//MPWB1K		G3(MP2)//MPW1K		G3(MP2)//MPWB1K	
	$A \times 10^{-18}$[a]	Ea/R[b]	$A \times 10^{-18}$[a]	Ea/R[b]	$A \times 10^{-19}$[a]	Ea/R[b]	$A \times 10^{-19}$[a]	Ea/R[b]
HR[c]	1.52 ± 0.11	-2571 ± 1.52	0.51 ± 0.56	-2098 ± 2.32	6.51 ± 0.54	-2616 ± 2	0.92 ± 0.18	-2204 ± 4

[a]Units: cm^3 $molecule^{-1} s^{-1}$;
[b]Units: K
[a,b] Arrhenius parameters obtained for the rate coefficients calculated using both Eckart's symmetrical and Wigner's tunneling methods.
The quoted uncertainties are 2σ (95% confidence limits) precision from the linear least squares fit of the kinetic parameters obtained for the reaction through each transition state.

Table 6. Tropospheric lifetimes of pinonaldehyde due to its reactivity with Cl atom and OH radical.

Tunneling Method	Tropospheric lifetime τ (h) at 300 K	
	Cl	OH
Eckart's symmetrical and Wigner's methods(G3(MP2)//MPWB1K)	5.8	3.2[a]
		2.9[b]
Eckart's Un-symmetrical (G3(MP2)//MPWB1K)	5.4	2[c]
		2.85 & 2.28[d]
Eckart's Un-symmetrical Net atmospheric life time OH & Cl		3.1

[a]Hallquist *et al.*[19]; [b]Alvarado *et al.*[20]; [c]Glasius *et al.*[21]; [d]Dash and B. Rajakuma[42]. The net atmospheric lifetime due to the reaction of pinonaldehyde with both Cl atoms [1.3×10^5 atom cm^{-3}] and OH radicals [1.0×10^6 radicals cm^{-3}].

In conclusion, as mentioned earlier, in case of all the tunneling corrections (Wigner's, Eckart's symmetrical and unsymmetrical tunneling corrections), the computed rate coefficients at 300 K with the G3(MP2)//MPWB1K theory are found to be in very good agreement with the experimentally reported value $(2.4 \pm 1.4) \times 10^{-10}$ cm^3 $molecule^{-1}$ s^{-1}at 295 ± 3 K by Nozière *et al.*,[22] and also with the estimated rate coefficient using SAR 3.3×10^{-10} cm^3 $molecule^{-1}$ s^{-1} by Atkinson *et al.*[58,59]

3.4 *Atmospheric lifetimes*

The atmospheric lifetime of volatile organic compounds released into the earth's atmosphere mainly depends on the rates of all process *viz.*, reaction with free radicals like OH, Cl and NO_3. Spicer *et al.*,[8] predicted that maximum chlorine atom levels occur shortly after sunrise with a peak concentration of 1.3×10^5 atoms cm^{-3} in both the remote marine boundary layer and coastal urban areas, and suggested that Cl atoms play an important role in the atmospheric chemistry. To calculate the global lifetime at room temperature, rates of all the reactions such as with OH radicals, NO_3 radicals, O_3, O (^1D and ^3P), Cl (^2P) atoms are requried. Also, the rates of the physical processes such as wet and dry depositions, and photo-physical parameters should be taken into account. Since all the information required for the calculation of global lifetime is not available, present calculations were restricted only to the estimation of local lifetime at room temperature due to its reactivity with Cl atoms alone. While calculating lifetime, we have used the chlorine concentration of 1.3×10^5atom cm^{-3}.[8] The computed atmospheric lifetime at due to the reactivity of the test molecule with Cl atom at G3(MP2)//MPWB1K level of theory with Wigner's method and Eckart's symmetrical methods are equal (5.8 h), and Eckart's unsymmetrical method is found to 5.4 h (table 6).

In conclusion, the estimated lifetime of pinonaldehyde due to its reactivity with Cl atom is a few hours at room temperature and therefore it is lost in the troposphere within this time after it is released. The atmospheric lifetimes are given in the table 6. The atmospheric lifetimes of pinonaldehyde due to its reactivity with OH radical are also included in this table for ready reference. It is obvious from this table that the lifetime of pinonaldehyde is governed both by OH radicals and Cl atoms in the marine boundary layer where the Cl atom concentration is 1.3×10^5 atoms cm^{-3}. However, the actual atmospheric lifetime of pinonaldehyde is due to its reactivity with both OH radicals and Cl atoms. Therefore, the cumulative or net atmospheric lifetime of the test molecule is calculated to be 3.1 h.

4. Conclusions

The H-abstraction reactions between pinonaldehyde and Cl atom were studied theoretically for the first time by using *ab initio* G3(MP2) and DFT based MPW1K and MPWB1K methods in the temperature range of 200-400 K. The results obtained with MPWB1K method seem to be more reliable and show good agreement with the experimental results when compared with the MPW1K method. The H-abstraction reactions with Cl atoms were found to have followed two reaction paths. One through the transition states lying higher in energy than the reactants and the other through the submerged transition state. The barrier heights and thermal properties such as enthalpy change, free energy change and entropy change show that the H-abstraction from the aldehydic site (-CHO) is both kinetically and thermodynamically more favourable than other –C sites. High quality experimental rate coefficients are necessary to have a good idea on the atmospheric lifetimes, and such experiments are planned in our laboratory.

Supplementary Information (SI)

The electronic supporting information can be seen at www.ias.ac.in/chemsci.

Acknowledgements

G.S. and B.R. are very grateful to the Ministry of Earth Sciences, Government of India for funding. We thank Mr. V. Ravichandaran, High performance computing centre (HPCE), Indian Institution of Technology Madras, Chennai, for providing us computational facility.

References

1. Guenther A, Hewitt C N, Erickson D, Fall R, Geron C, Graedel T, Harley P, Klinger L, Lerdau M and McKay W A 1995 *J. Geophys. Res.* **100** 8873
2. Guenther A, Geron C, Pierce T, Lamb B, Harley P and Fall R 1996 *Atmos. Environ.* **34** 2205
3. Fall R and Hewitt C N (Ed.) 1999 In *Reactive Hydrocarbons in the Atmosphere* (San Diego: Academic Press) p. 41
4. Fuentes J D, Lerdau M, Atkinson R, Baldocchi D, Bottenheim J W, Ciccioli P, Lamb B, Geron C, Gu L, Guenther A, Sharkey T D and Stockwell W 2000 *B. Am. Met. Soc.* **81** 1537
5. Geron C, Rasmussen R, Arnts R R and Guenther A 2000 *Atmos. Environ.* **34** 1761
6. Atkinson R, Baulch D L, Cox R A, Crowley J N, Hampson R F, Hynes R G, Jenkin M E, Rossi M J and Troe J 2006 *Atmos. Chem. Phys.* **6** 3625
7. Singh H B, Thakur A N, Chen Y E and Kanakidou M 1996 *Geophys. Res. Lett.* **23** 1523
8. Spicer C W, Chapman E G, Finlayson-Pitts B J, Plastridge R A, Hubbe J M, Fast J D and Berkowitz C M 1998 *Nature* **394** 353
9. Platt U, Allan W and Lowe D 2004 *Atmos. Chem. Phys.* **4** 2393
10. Wingenter O W, Kubo M K, Blake N J, Smith Jr. T W, Blake D R and Rowland F S 1996 *J. Geophys. Res.* **101** 4331
11. Graedel T E and Keene W C 1995 *Global Biogeochem. Cycl.* **9** 47
12. DeHaan D O, Brauers T, Oum K, Stutz J, Nordmeyer T and Finlayson-Pitts B J 1999 *Int. Rev. Phys. Chem.* **18** 343
13. Keene W C 1995 In *Inorganic C1 Cycling in the Marine Boundary Layer: A Review* In *Naturally Produced Organohalogens* A Grimvall A and E W B de Leer (Eds.) (Dordrecht, The Netherlands: Kluwer Academic) p. 363
14. Keene W C, Jacob D J and Fan S M 1996 *Atmos. Environ.* **30** R1–R3
15. DeMore W B, Sander S P, Golden D M, Hampson R F, Kurylo M J, Howard C J, Ravishankara A R, Kolb C E and Molina M J 1997 In *Chemical Kinetics a Photochemical Data for Use in Stratospheric Modeling* Evaluation Number 12 (California Institute of Technology, Pasadena, CA: J P L Publication) pp. 97-4
16. Atkinson R, Baulch D L, Cox R A, Hampson Jr. R F, Kerr J A, Rossi M J and Troe J 1997 *J. Phys. Chem. Ref. Data* **26** 521
17. Atkinson R J 1997 *J. Phys. Chem. Ref. Data* **26** 215
18. Davis M E, Talukdar R K, Notte G, Ellison G B and Burkholder J B 2007 *Environ. Sci. Technol.* **41** 3959
19. Hallquist M, Wängberg I and Ljungström E 1997 *Environ. Sci. Technol.* **31** 3166
20. Alvarado A, Arey J and Atkinson R 1998 *J. Atmos. Chem.* **31** 281
21. Glasius M, Galogirou A, Jensen N R, Hjorth J and Nielsen C J 1997 *Int. J. Chem. Kinet.* **29** 527
22. Nozière B, Spittler M, Ruppert L, Barnes I, Becker K H, Pons M and Wirtz K 1999 *Int. J. Chem. Kinet.* **31** 291
23. Lynch B J, Fast P L, Harris M and Truhlar D G 2000 *J. Phys. Chem. A* **104** 4811
24. Zhao Y and Truhlar D G 2004 *J. Phys. Chem. A* **108** 6908
25. Frisch M J *et al.* 2010 *Gaussian 09, Revision B.01* (Gaussian, Inc.: Wallingford CT
26. Zhao Y, Schultz N E and Truhlar D G 2006 *J. Chem. Theor. Comput.* **2** 364
27. Chandra A K 2012 *J. Mol. Model.* **18** 4239
28. Fernandez-Ramos A, Miller J A, Klippenstein S J and Truhlar D G 2006 *Chem. Rev.* **106** 4518
29. Curtiss L A, Redfern P C, Raghavachari K, Rassolov V and Pople J A 1999 *J. Chem. Phys.* **110** 4703
30. Dennington I I R, Keith T, Millam J, Eppinnett K, Hovell W L and Gilliland R 2003 *GaussView, Version 3.09* (Semichem, Inc.: Shawnee Mission, KS)
31. Wright M R 1999 In *Fundamental Chemical Kinetics and Exploratory Introduction to the Concepts* (Chichester UK: Ellis Horwood)
32. Ralchenko Y, Jou F C, Kelleher D E, Kramida A E, Musgrove A, Reader J, Wiese W L and Olsen K 2007 *NIST Atomic Spectra Database, version 3.1.2* (National Institute of Standards and Technology: Gaithersburg, MD)
33. Wigner E P Z 1932 *Phys. Chem. B* **19** 203
34. Eckart C 1930 *Phys. Rev.* **35** 1303
35. Johnston H S and Heicklen J 1962 *J. Phys. Chem.* **66** 532
36. Louis F, Gonzalez C A, Huie R E and Kurylo M J 2000 *J. Phys. Chem. A* **104** 8773
37. Ali M A and Rajakumar B 2010 *J. Comput. Chem.* **31** 500
38. Ali M A and Rajakumar B 2010 *J. Mol. Struct: THEOCHEM* **949** 73
39. Kaliginedi V, Ali M A and Rajakumar B 2012 *Int. J. Quantum Chem.* **112** 1066
40. Ali M A and Rajakumar B 2011 *Int. J. Chem. Kinet.* **43** 418
41. Ali M A, Upendra B and Rajakumar B 2011 *Chem. Phys. Lett.* **511** 440
42. Dash M R and Rajakumar B 2012 *J. Phys. Chem. A* **116** 5856
43. Korchowiec J, Kawahara S I, Matsumura K, Uchimara T and Surgie M 1999 *J. Phys. Chem. A* **103** 3548
44. Chandra A K and Uchimaru T 2000 *J. Phys. Chem. A* **104** 8535
45. Alvarez-Idaboy J R, Cruz-Torres A, Galano A and Ruiz-Santoyo M E 2004 *J. Phys. Chem. A* **108** 2740
46. Zhang M, Lin Z and Song C 2007 *J. Chem. Phys.* **126** 34307
47. Chuang Y and Truhlar D G 2000 *J. Chem. Phys.* **112** 1221
48. Gruber-Stadler M, Mühlhäuser M, Sellevåg S R and Nielsen C J 2008 *J. Phys. Chem. A* **112** 9
49. Beukes J A, D'Anna B, Bakken V and Nielsen C J 2000 *Phys. Chem. Chem. Phys.* **2** 4049
50. Alvarez-Idaboy J R, Mora-Diez N, Boyd R J and Vivier-Bunge A 2001 *J. Am. Chem. Soc.* **123** 2018

51. Alvarez-Idaboy J R, Mora-Diez N and Vivier-Bunge A 2000 *J. Am. Chem. Soc.* **122** 3715
52. Galano A, Alvarez-Idaboy J R, Ruiz-Santoyo Ma Esther and Vivier-Bunge A 2005 *J. Phys. Chem. A* **109** 169
53. Vereecken L and Peeters J 2002 *Phys. Chem. Chem. Phys.* **4** 467
54. Wang Y, Liu J-y, Li Zs, Wang L, Wu J-y and Sun C-c 2006 *J. Phys. Chem. A* **110** 5853
55. Sun H and Law C K 2010 *J. Phys. Chem. A* **114** 12088
56. Gao H, Liu J-y and Sun C-c 2009 *J. Chem. Phys.* **130** 224301
57. Srinivasulu G and Rajakumar B 2013 *J. Phys. Chem. A* **117** 4534
58. Aschmann S M and Atkinson R 1995 *Int. J. Chem. Kinet.* **27** 613
59. Tyndall G S, Orlando J J, Wallington T J, Dill M and Kaiser E W 1997 *Int. J. Chem. Kinet.* **29** 43